Nr 9 (623—686, I—XVIII) WRZESIEŃ 2014 Tom LIX

POLIMERY

CZASOPISMO POŚWIĘCONE CHEMII, TECHNOLOGII i PRZETWÓRSTWU POLIMERÓW

Modified nanosilica-filled polypropylene composites with glycidyl methacrylate grafted ethylene/*n*-octene copolymer as compatibilizer*)

Maciej Studziński[1)], Regina Jeziórska[1), **)], Agnieszka Szadkowska[1)], Maria Zielecka[1)]

DOI: dx.doi.org/10.14314/polimery.2014.625

Abstract: Modified nanosilica-filled polypropylene composites were manufactured by *in situ* reactive processing. The key issue lies that amine functional groups of silica nanoparticles reacted with glycidyl methacrylate grafted ethylene/*n*-octene copolymer (EOC-*g*-GMA) in order to improve nanofiller dispersion and increase compatibility between silica and PP matrix. Taking the advantages of rubber-type grafted polymer (ethylene/*n*-octene copolymer) and reactive compatibilization with NH_2-SiO_2, a synergetic toughening effect was observed for the PP composites. Just very low concentrations of silica nanoparticles (2 wt %) and EOC-*g*-GMA (4 or 6 wt %) were sufficient to increase significantly notched impact strength and elongation at break of PP. On the contrary, tensile strength of the composites is slightly decreased. Improved dispersion of silica and increased compatibility between silica and PP matrix were observed in the presence of EOC-*g*-GMA. The crystalline features of PP have not been influenced greatly by addition of both modified silica and compatibilizer. However, the spherulite size of PP dramatically decreased in all composites. The thermal stability of the composites was significantly better compared to PP. Improved stiffness due to increased both storage and loss moduli indicating very good interfacial adhesion was observed.

Keywords: spherical silica nanoparticles, composites, polypropylene, compatibilizers.

Kompozyty polipropylen/nanokrzemionka z udziałem EOC-*g*-GMA jako kompatybilizatora

Streszczenie: Polipropylen modyfikowany nanokrzemionką otrzymywano *in situ* w procesie reaktywnego wytłaczania. W wyniku reakcji grup aminowych, wprowadzonych do nanocząstek krzemionki (NH_2-SiO_2), z metakrylanem glicydylu szczepionym na kopolimerze etylen/*n*-oktan (EOC-*g*-GMA) polepszyła się dyspersja nanonapełniacza w osnowie polipropylenowej oraz zwiększyła się kompatybilność układu krzemionka/PP. Już mała zawartość nanokrzemionki (2 % mas.) i EOC-*g*-GMA (4—6 % mas.) powodowały zwiększenie udarności i wydłużenia przy zerwaniu, natomiast wytrzymałość na rozciąganie zmieniała się tylko w niewielkim stopniu. Obecność w układzie napełniacza i kompatybilizatora nie

[1)] Industrial Chemistry Research Institute; ul. Rydygiera 8, 01-793 Warszawa, Poland.

*) Material contained in this article was presented at the MoDeSt Workshop 2013, Warsaw, Poland, 8—10 September 2013.

**) Corresponding author; e-mail: regina.jeziorska-dn@ichp.pl

wpłynęła w istotnym stopniu na strukturę krystaliczną PP, ale we wszystkich kompozytach znacznie zmniejszyły się rozmiary sferolitów PP. Stabilność termiczna kompozytów była znacznie większa niż osnowy polimerowej PP. Zwiększenie sztywności kompozytu, wyrażone wzrostem modułu zachowawczego i modułu stratności, wskazuje na bardzo dobrą adhezję na granicy faz. Zaobserwowane zmiany są efektem synergii NH_2-SiO_2 z EOC-*g*-GMA.

Słowa kluczowe: nanokrzemionka sferyczna, kompozyty, polipropylen, kompatybilizatory.

Among polyolefins polypropylene (PP) is one of the most widely used commodity thermoplastic polymers due to its attractive properties and low cost. It is well known that the mechanical properties of PP can be improved when inorganic fillers are well dispersed in PP matrix [1—4]. One big issue concerning dispersion of inorganic fillers in PP is the hydrophobic nature of the polymer, which prevents a good interfacial adhesion with hydrophilic fillers. Several attempts have been made to improve the dispersion of filler in the polymer matrix such as the incorporation of coupling agents and compatibilizers during processing or prior to melt mixing process [5, 6]. The compatibilizer should be miscible with the polypropylene matrix and should include a certain amount of polar functional groups [7—11]. Maleic anhydride grafted PP (PP-*g*-MAH) or acrylic acid grafted PP (PP-*g*-AA) are the most commonly used compatibilizers for PP [12, 13]. This issue can be also overcome by chemical surface treatment of inorganic fillers and *in situ* polymerization, etc. [6, 14, 15]. There are two advantages regarding chemical surface modification of nanofillers. One is the stabilization of nanoparticles towards agglomeration and the other is improvement in the compatibility between particle surface and polymer matrix.

Spherical silica particles exhibit hydrophilic nature and very high surface energy due to their extremely high surface area per unit weight and the numerous silanol groups on the surface due to their manufacturing process [16]. These characteristics lead to the formation of aggregates and particle-particle interactions between the silica particles in non-polar liquids [17]. Thus in the case of a non-polar polymer, such as PP, compatibilizers as well as modified silica should be used in order to achieve a satisfactory dispersion of the filler in the polymer matrix.

In our previous work, we found that silica filled-low density polyethylene composites showed improved mechanical properties such as tensile strength, Young's modulus and impact strength. These properties are mainly affected by the amount and size of silica nanoparticles. The addition of modified silica and glycidyl methacrylate grafted ethylene/*n*-octene copolymer as a compatibilizer resulted in further enhancement of mechanical properties due to the better dispersion of silica nanoparticles and increased compatibility between silica and the PE-LD matrix. Both permitted a much more efficient transfer of stress from the polymer matrix to the silica nanoparticles [18]. From FT-IR results it was confirmed, that the interactions between amine groups of NH_2-SiO_2 and the epoxy groups of EOC-*g*-GMA are possible and probably take place according to Scheme A.

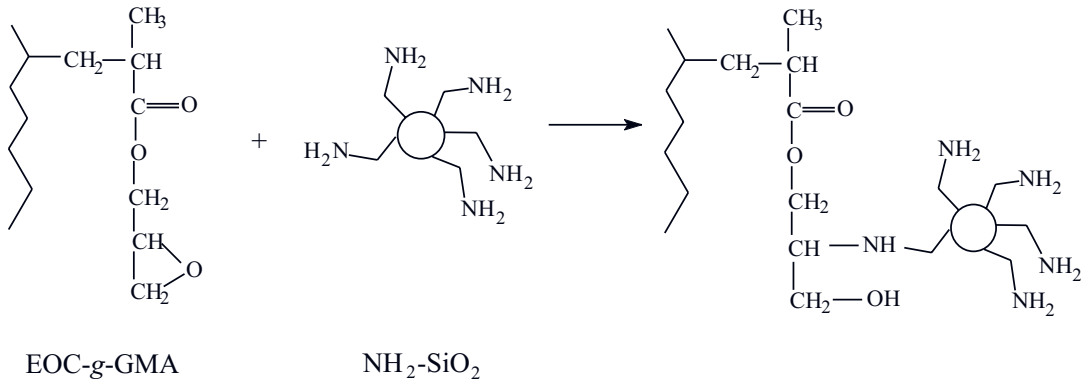

Scheme A

Therefore, in this paper, the effects of introduction glycidyl methacrylate grafted rubber-type ethylene/*n*-octene copolymer (EOC-*g*-GMA) into the amine functionalized silica-filled polypropylene composites (PP/NH_2-SiO_2) on morphology, thermal and mechanical properties were investigated. For that purpose, the following properties were characterized and discussed, the quality of silica nanoparticles dispersion in PP matrix, the crystalline behaviour, thermal and mechanical properties of PP/NH_2-SiO_2 composites. It is expected that the amine groups of silica nanoparticles can react with epoxy functional groups of EOC-*g*-GMA used as compatibilizer, leading to a finer dispersion of the individual silica nanoparticles in the PP matrix. Moreover, the composites prepared in this way would take the advantages of rub-

ber-type grafted polymer and interfacial reactive compatibilization with NH_2-SiO_2 nanoparticles. Ethylene/*n*-octene copolymer modified with glycidyl methacrylate, to the best of our knowledge, has not been used in the preparation of polypropylene composites.

EXPERIMENTAL PART

Materials

Isotactic polypropylene homopolymer (PP) granules were supplied by Orlen Polyolefins (Moplen HP456H). The melt flow rate (*MFR*) of this PP is 1.3 g/10 min (ISO 1133).

The glycidyl methacrylate (GMA) was used for melt grafting onto rubber-type polyolefine — ethylene/*n*-octene copolymer (EOC, Engage 8200, *MFR* 5.0 g/10 min at 190 °C, from DuPont Dow Elastomers). Grafted copolymer (EOC-*g*-GMA), *MFR* 2.8 g/10 min at 190 °C, containing 0.6 wt % glycidyl methacrylate was prepared by melt blending according to the procedure published elsewhere [19, 20] and used as a compatibilizer for composites in concentrations of 4 or 6 wt %.

Modified silica nanoparticles preparation and testing

Spherical silica having 0.35 wt % of amine functional groups (NH_2-SiO_2) with an average primary particle size of 60 nm and specific surface area equal to 260 m^2/g was synthesized according to the sol-gel process published elsewhere [21, 22]. In brief, ethyl alcohol (reagent grade, POCH S.A.), aqueous ammonia (reagent grade, 25 wt %, density 0.91 g/cm^3, POCH S.A.) and distilled water were mixed to obtain the reaction mixture. The initial pH of the reaction mixture was measured using pH-meter Schott Instruments LAB 850. All syntheses were carried out at room temperature (23 °C). Tetraethoxysilane (TES 28, Wacker Chemie) distilled immediately before use for the preparation of nanoparticles, used as alkoxysilane precursor was added to the reaction mixture stirred with constant speed during 2 hours. The reaction mixture containing TEOS/EtOH/H_2O in the molar ratios 0.023/0.500/0.477 was used in the synthesis with the initial pH range from 10.4 to 11.3 and the final pH range was 7.5—10.8, with further *in situ* modification using γ-aminopropylotriethoxysilane (Momentive Performance Materials). The process of silica nanoparticles modification is given by the following reaction:

The modified silica nanoparticles were dried in an oven dryer for 2 h at 50— 90 °C. Photon correlation spectroscopy (PCS) was used to evaluate particle size and particle size distribution of resulting sol. The measurements were performed using a Malvern apparatus (Zetasizer Nano ZS). The results were registered in the form of the particle size distribution curve. The resulting peak was analyzed using the averaged number method.

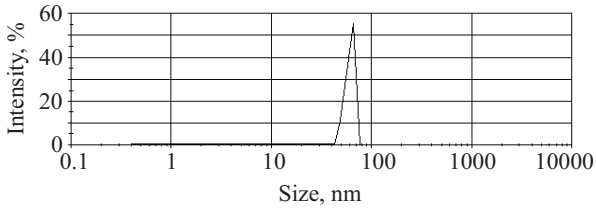

Fig. 1. The particle size distribution of NH_2-SiO_2 nanoparticles of average size 60 nm

In Fig. 1 the particle size distribution curve of NH_2-SiO_2 nanoparticles is shown. The developed synthesis method allows preparation silica nanoparticles characterized by an almost uniform particle size, which is relating to the selection of the sol-gel process parameters. The monomodal particle size distribution and very low dispersion of particle size were observed for homogeneous sol of silica obtained by sol-gel process. The specific surface area of silica nanoparticles was measured by BET–N2 sorption method using Gemini 2370 V3.02 apparatus. FT-IR spectra of the nanosilica in the mid-IR range were recorded using PERKIN-ELMER System 2000 spectrometer both in KBr pellets in transmission mode and KRS crystal in reflection mode. The IR spectra of the final silica did not reveal any presence of organic material, especially in the region of stretching vibrations C–H at 2900 cm^{-1}, thus confirming the completion of the hydrolysis reaction of Si–O–C bonds in alkoxysilane precursors [18, 23]. The amine groups content was determined based on nitrogen content measurement by Kiejdahl method. Scanning electron microscopy (SEM) was performed using a JEOL JSM-6490LV operating in the high vacuum mode at accelerating voltage of 15 kV to evaluate morphology of silica nanoparticles. The SEM micrograph revealed spherical shape and uniform size of synthesized silica nanoparticles (see Fig. 2).

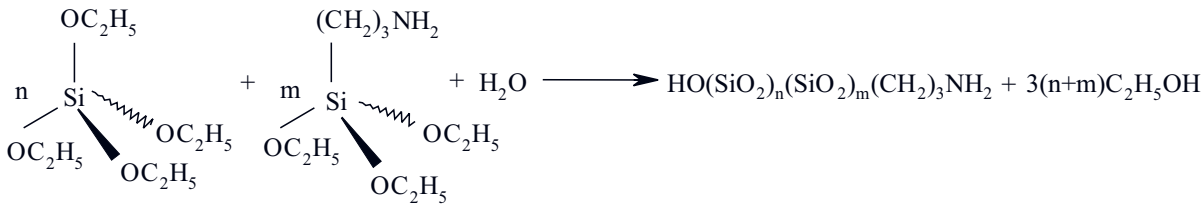

Scheme B

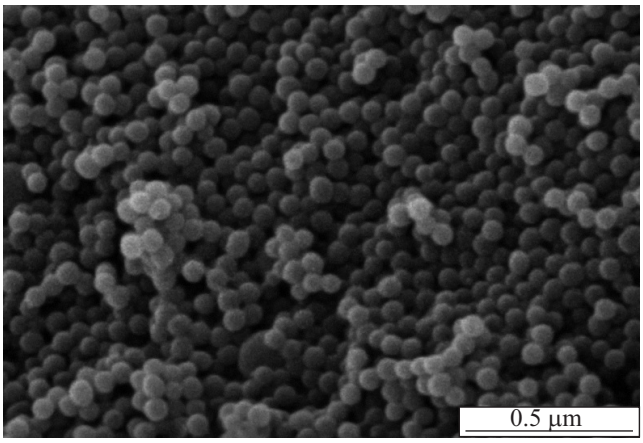

Fig. 2. SEM micrograph of NH_2-SiO_2 nanoparticles

Composites preparation

Prior to use, polypropylene granules and silica nanoparticles were dried in an oven at 80 °C for 12 h. The composites were prepared using melt blending in a Berstorff twin screw co-rotating extruder (ZE-25x33D). The diameter of the screws was 25 mm and the length/diameter ratio (*L*/*D*) was 33. Different screw elements along the screw worked in order to induce polymer melting and achieve a finer dispersion of the nanoparticles in the polymer melt [24]. The three mixing sections enhanced the compounding and also increased the residence time of the mixture in the barrel. The barrel pressure in these parts, as well as at the metering section before the die, could be increased. The extruder also had a vacuum degassing port to remove any moisture traces or other volatile products formed during compounding. EOC-*g*-GMA and PP granules were first premixed prior to compounding process. All the materials (PP, PP/EOC-*g*-GMA, NH_2-SiO_2) were fed into the throat of the extruder using separate gravimetric feeders. The process temperature was ranged from 175 °C near the hopper to 215 °C at the die. The screw speed was 250 rpm. The melt temperature and pressure were continuously recorded during compounding. After compounding, the material was extruded from the die, which had two cylindrical nozzles of 4 mm diameter. Then was immersed immediately into a cold-water bath (20 °C) and pelletized with an adjustable rotating knife, located behind the water bath, into 5 mm pellets.

Composite characterization

— The dispersion quality of NH_2-SiO_2 nanoparticles in PP matrix and the morphology of fracture surfaces was examined using scanning electron microscopy (SEM, JSM-6490LV).

— The spherulites structure and size of matrix in neat PP and PP/NH_2-SiO_2 composites were also studied using SEM. The samples were etched before SEM examination in an etchant composed of 1 wt % of potassium permanganate in a mixture of concentrated sulphuric acid and phosphoric acid in a 3:2 volume ratio. The etch time was 5 h at room temperature. After etching the samples were cleaned in distilled water and acetone and then dried. All specimens were sputtered with a thin gold film prior to SEM examination.

— Differential scanning calorimetry (DSC) was performed using a Perkin Elmer instrument (DSC-7) under nitrogen atmosphere. The following procedure was used: each sample was heated from 40 to 200 °C at the heating rate of 10 deg/min and then held at 200 °C for 5 min to ensure an identical thermal history. The specimen was subsequently cooled down to room temperature at a cooling rate of 10 deg/min.

— Thermogravimetric analysis (TGA) was carried out under air, using a Mettler Toledo TGA/SDTA 851e equipment from room temperature to 600 °C at a heating rate of 10 deg/min.

— The dynamic mechanical thermal properties of samples were tested using a dynamic mechanical analyzer, model Rheometrics RDS 2. The torsion method was used with a frequency of 1 Hz, a strain level of 0.1 % in the temperature range of -100 to 150 °C. The heating rate was 3 deg/min. The testing was performed using rectangular bars measuring approximately 38 × 10 × 2 mm, prepared by injection molding. The storage and loss moduli (G', G''), and the loss factor, tan δ, were obtained.

— The tensile test was performed using an Instron Series 4505 universal testing machine according to ISO 527 (dog-bone-shaped specimens) at room temperature. The crosshead speed was 50 mm/min. Samples were prepared by injection molding using an Arburg 420 M single screw injection machine (Allrounder 1000-250) containing five different heating zones. The temperatures of these were 175/190/200/220/230 °C, from the feeding zone to the die, while the mold was cooled with water at 35 °C. At least of 5 specimens for each composite were tested in order to estimate the precision of the reported data.

— Charpy notched impact tests were carried out using a Zwick hammer for impact test according to ISO 179 at room temperature.

RESULTS AND DISCUSSION

Dispersion of nanoparticles

Figure 3 shows SEM micrographs of PP/NH_2-SiO_2 (98/2) composites as a function of compatibilizer (EOC-*g*-GMA) content. The images of the fractured surface of the composites show rough fracture surface with different tendency towards the crack propagation. It is clear from Fig. 3, that composites containing EOC-*g*-GMA show smoother fractured surface compared to that one without. Such a type of rough surface morphology can be related to the improvement in mechanical properties [25]. The SEM images showed that all the samples contain agglomerates. However, the tendency to

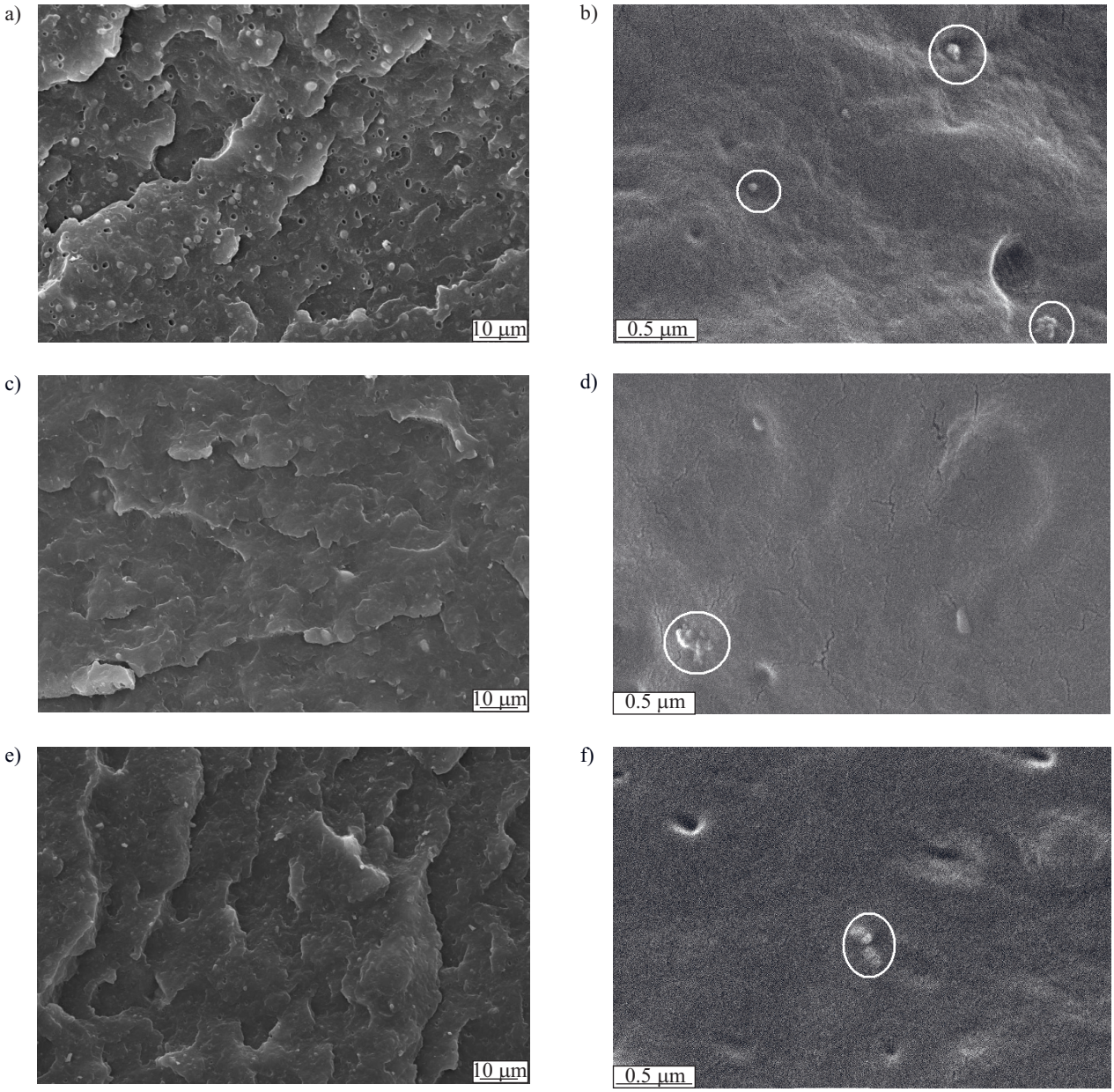

Fig. 3. SEM micrographs of PP/NH_2-SiO_2 composites: (a, b) without EOC-*g*-GMA, (c, d) 4 wt % of EOC-*g*-GMA, (e, f) 6 wt % of EOC-*g*-GMA

form agglomerates decreases in the presence of EOC-*g*-GMA. Conversely, the PP/NH_2-SiO_2 (98/2) composite without EOC-*g*-GMA shows more agglomerates and particles clusters as marked in the images. Comparing the composites with compatibilizer, less agglomerates were observed in the presence of lower EOC-*g*-GMA content, suggesting better compatibility. It can be concluded that EOC-*g*-GMA improves the compatibility between silica nanoparticles and the PP matrix due to their uniform dispersion.

Crystallization behavior of composites

The effect of compatibilizer's content on crystallization behavior of amine functionalized silica-filled PP composites was determined by DSC measurements.

Figures 4 and 5 show the second heating and cooling DSC curves of PP and investigated silica-filled PP composites. The important data obtained are listed in Table 1.

T a b l e 1. Thermal transition properties (second run) of PP, and PP/NH_2-SiO_2 (98/2) composites, differing in EOC-*g*-GMA content, determined by DSC method

Symbol of sample	T_m, °C	T_c, °C	X_c*), %
PP	166.4	115.4	25.3
PP/NH_2-SiO_2/EOC-*g*-GMA 0 wt %	163.9	115.1	25.2
PP/ NH_2-SiO_2/EOC-*g*-GMA 4 wt %	164.7	115.3	26.3
PP/ NH_2-SiO_2/EOC-*g*-GMA 6 wt %	163.3	115.0	24.3

*) Degree of crystallinity calculated using AH of PP equilibrium crystals 209 J/g; T_m — melting temperature, T_c — crystallization temperature, X_c — crystallinity.

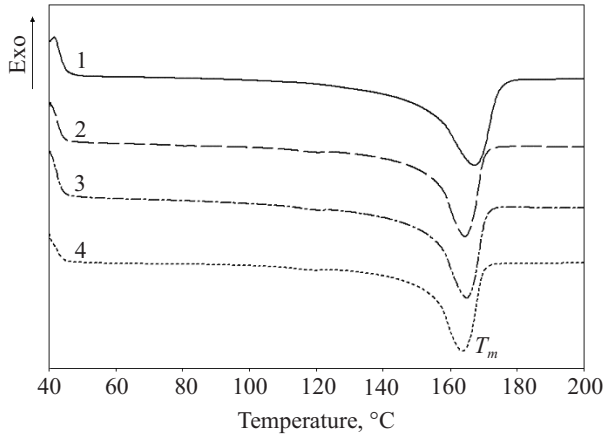

Fig. 4. DSC curves of PP and PP/NH_2-SiO_2 composites, differing in EOC-*g*-GMA content: 1 — PP, 2 — without EOC-*g*-GMA, 3 — 4 wt % of EOC-*g*-GMA, 4 — 6 wt % of EOC-*g*-GMA; second heating

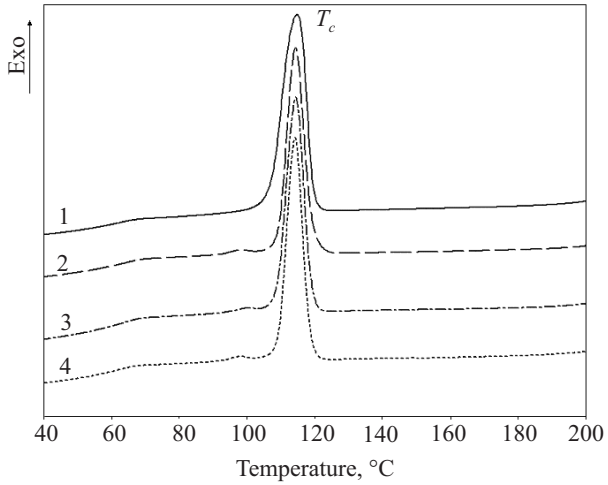

Fig. 5. DSC curves of PP and PP/NH_2-SiO_2 composites, differing in EOC-*g*-GMA content: 1 — PP, 2 — without EOC-*g*-GMA, 3 — 4 wt % of EOC-*g*-GMA, 4 — 6 wt % of EOC-*g*-GMA; cooling run

It is clear from the results, that the melting temperatures (T_m) of PP matrix in all composites are slightly lower compared to neat PP. However, the addition of 4 wt % of EOC-*g*-GMA slightly increases T_m compared to the PP/NH_2-SiO_2 composite. As expected, the melting temperature is shifted to lower temperature as rubber-type grafted polymer (EOC-*g*-GMA) content in the composite increases. Moreover, the addition of NH_2-SiO_2 shows no effect on the crystallinity of PP matrix. However, the introduction of 4 wt % of EOC-*g*-GMA increases the polymer crystallinity from 25.2 to 26.3 %. Consequently, the crystallinity of the composites decreases with increased compatibilizer content. Besides, the addition of modified silica as well as compatibilizer shows no effect on the crystallization temperatures (T_c) of PP. However, the highest value of T_c is observed for 4 wt % of EOC-*g*-GMA content. Based on these results, it can be concluded that the crystalline features of PP have not been influenced greatly by the addition of both modified nanosilica and compatibilizer. These results are in good agreement with previous studies [26— 28].

The SEM micrographs in Fig. 6 show spherulites features of neat PP matrix and PP/NH_2-SiO_2 composites. It can be clearly seen that neat PP shows typical three-dimensional spherulites with clear boundaries. On the contrary, no spherulite structure is observed in all PP/NH_2-SiO_2 composites. This result should be attributed to the presence of nanoparticles preventing the growth of PP crystals due to small interparticle distances.

Thermogravimetric analysis

The TGA curves of the neat PP and silica-filled composites in an air atmosphere are displayed in Table 2. The onset (T_{on}), maximum (T_{max}) and thermooxidative decomposition temperatures at 10 % (T_{10}) and 50 % weight loss (T_{50}) are evaluated from the TGA curves, as listed in Table 2. It was found that the presence of silica as well as EOC-*g*-GMA significantly altered the degradation mechanism of PP. It was observed that the presence of NH_2-SiO_2 particles greatly improved thermal properties of PP composites due to the 3—12 °C higher thermooxidative decomposition temperatures. Moreover, the introduction of EOC-*g*-GMA into the PP/NH_2-SiO_2 composite further enhanced thermal properties of PP matrix, indicated by 4—13 °C higher T_{50} and about 12—24 °C higher T_{max}. An increase in thermal stability of silica-filled PP composites may be explained by the formation of the PP-silica nanoparticles network by the physical cross-linking of PP via silica nanoparticles; this causes the whole system to be stabilized due to the thermal motions of the PP chains being restricted.

Dynamic-mechanical properties

In order to evaluate the effect of NH_2-SiO_2 nanoparticles as well as EOC-*g*-GMA on the PP matrix, thermo-mechanical properties were also measured. Due to the

T a b l e 2. Thermal analysis of PP and PP/ NH_2-SiO_2 (98/2) composites, differing in EOC-*g*-GMA content, determined by TGA method

Symbol of sample	T_{on}, °C	$T_{10\,\%}$, °C	$T_{50\%}$, °C	T_{max}, °C	Weight loss, %
PP	279.1	292.2	341.6	351.8	100.0
PP/NH_2-SiO_2/EOC-*g*-GMA 0 wt %	276.5	290.5	344.7	364.4	98.6
PP/NH_2-SiO_2/EOC-*g*-GMA 4 wt %	274.0	288.0	345.3	363.5	98.2
PP/NH_2-SiO_2/EOC-*g*-GMA 6 wt %	272.2	293.3	354.6	375.3	98.1

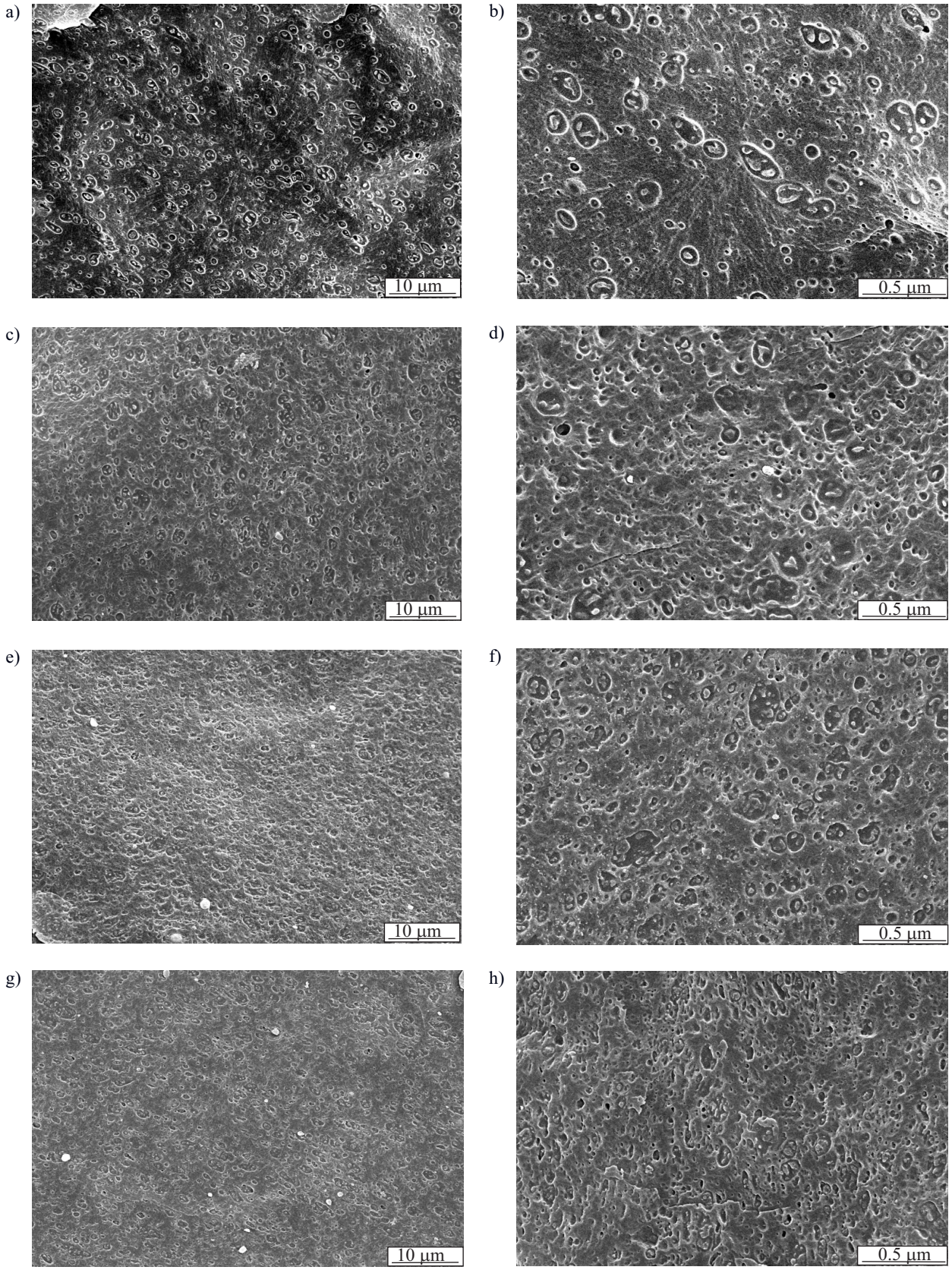

Fig. 6. Spherulite structure in neat PP (a, b) and PP/NH_2-SiO_2 composites: (c, d) without EOC-*g*-GMA, (e, f) 4 wt % of EOC-*g*-GMA, (g, h) 6 wt % of EOC-*g*-GMA

very high surface area of the nanoparticles in the PP composites, the applied stresses are expected to be easily transferred from the matrix onto the silica particles, resulting in an enhancement of the mechanical properties. It was reported that good dispersion quality and strong interfacial interactions between filler particles and poly-

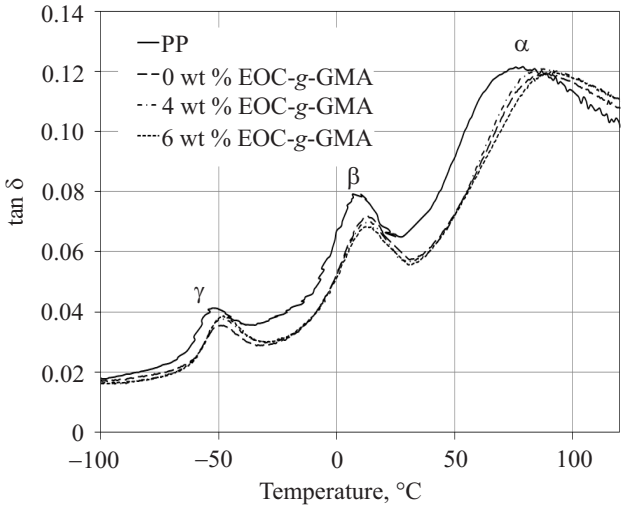

Fig. 7. Mechanical loss factor tan δ as a function of temperature for all samples

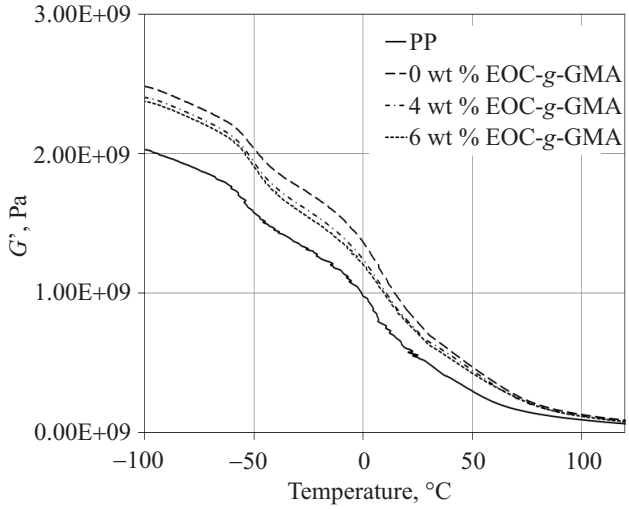

Fig. 8. Storage modulus (*G'*) as a function of temperature for all samples

mer matrix will restrict the movement of matrix molecules, resulting in an increase of glass transition temperature (T_g) [4, 29].

Figure 7 shows the mechanical loss factor (tan δ), as a function of temperature for all samples, because tan δ is a sensitive indicator of molecular motions and phase transition. It can be seen that tan δ curves of all samples exhibit three relaxation peaks within selected temperature range. The first peak around -52 °C for PP and around -49 °C for the composites corresponds to the γ relaxation process, predominantly of amorphous origin. This relaxation is typical for the joint movements of chains containing three or more methylene groups (units) in the main chain [30]. The intensity of the γ relaxation is usually associated with the amorphous region of semicrystalline polymers. Therefore, the decrease in the intensity of γ relaxation of the silica-filled composites, can be attributed to the decrease in the quantity of the amorphous phase.

The second peak around 7 °C for neat PP and around 12 °C for the composites corresponds to the glass transition of amorphous PP (β relaxation). Moreover, the addition of 4 wt % of EOC-*g*-GMA clearly shifted this peak to higher temperature compared to the PP/NH_2-SiO_2 composite. Evidently, all composites show decreased β transition peak intensity compared to PP matrix. Besides, the composite containing 6 wt % of EOC-*g*-GMA shows the lowest intensity of β transition peak.

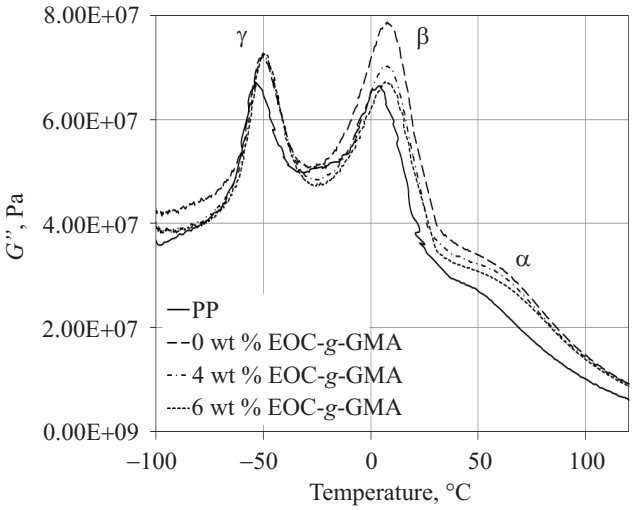

Fig. 9. Loss modulus (*G''*) as a function of temperature for all samples

The third transition peak around 76 °C for neat PP and around 90 °C for the composites is attributed to α relaxation of crystalline PP due to the crystal-crystal slippage motion [31]. It is clear that the addition of 6 wt % of compatibilizer shifted this peak to higher temperature compared to the PP/NH_2-SiO_2 composite. The broadness of this peak may indicate a distribution of lamellar thickness of PP crystals. Therefore, chain mobility occurs at

T a b l e 3. DMTA results for PP and PP/NH_2-SiO_2 composites, differing in EOC-*g*-GMA content

Symbol of sample	*G'*, MPa at *T* = 23 °C	*G''*, MPa at *T* = 23 °C	tan δ (peak position), °C		
			α	β	γ
PP	580	363	76.0	7.2	-52.5
PP/NH_2-SiO_2/EOC-*g*-GMA 0 wt %	878	576	87.1	12.8	-49.7
PP/NH_2-SiO_2/EOC-*g*-GMA 4 wt %	812	530	86.3	13.1	-48,7
PP/NH_2-SiO_2/EOC-*g*-GMA 6 wt %	798	510	90.9	12.7	-48.3

higher temperature as crystallite thickness increases. The position and intensity of the α relaxation maximum is usually connected with crystallites' thickness and crystallinity level, respectively [31].

Figures 8 and 9 show the storage and loss moduli (*G'*, *G''*) as a function of temperature for all samples. The storage and loss moduli (*G'*, *G''*) at 23 °C, and relaxation temperatures (T_α, T_β and T_γ) of all samples are summarized in Table 3.

One can see from the results, that the introduction of NH_2-SiO_2 nanoparticles into PP significantly improves the storage and loss moduli of composites indicating higher stiffness of the material. As showed in Table 3, the addition of NH_2-SiO_2 to PP improved *G'* and *G''* at 23 °C about 50 % and 60 %, respectively. Silica could hinder the chain motion of PP, which would improve the moduli. As a result of these changes, the storage modulus of the interface is higher than that of the free part. Moreover, the storage and loss moduli slightly decrease with increased compatibilizer content. However, the values of both moduli are still significantly higher in comparison with neat PP. One possible explanation of this fact could be that rubber-type grafted polymer such as ethylene/*n*-octene copolymer exhibits very low molecular weight and viscosity compared to the PP. These results are in a good agreement with mechanical properties (see Table 4).

The β transition temperatures of PP/NH_2-SiO_2 composites are significantly higher compared to neat PP. Evidently, the PP/NH_2-SiO_2 composite containing 4 wt % of EOC-*g*-GMA shows the highest temperature of β transition relaxation amongst all the samples. This is related to increased interfacial interactions between PP matrix and NH_2-SiO_2 nanoparticles. DMTA results can be attributed to different dispersion quality of surface modified silica nanoparticles and slightly decreased crystallinity of PP matrix in the composites.

Mechanical properties

It is expected that PP/NH_2-SiO_2 composites containing EOC-*g*-GMA take the advantages of rubber-type grafted polymer and interfacial reactive compatibilization with NH_2-SiO_2 nanoparticles. For having better understanding of the effect of them, normalized mechanical properties of PP and its composites are illustrated in Fig. 10 and summarized in Table 4.

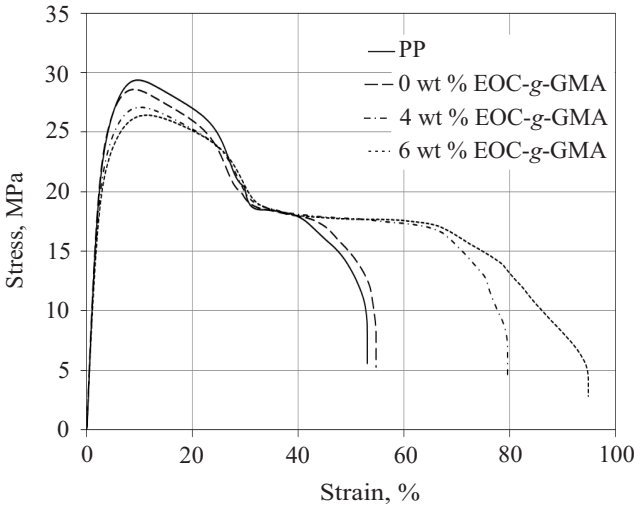

Fig. 10. Stress-strain curves of PP and PP/NH_2-SiO_2 composites

Obviously, the proposed route works. In comparison with neat PP as well as PP/NH_2-SiO_2 (98/2) composite, impact strength and elongation at break of composites containing EOC-*g*-GMA are definitely improved, and the composite containing 6 wt % EOC-*g*-GMA has the highest toughness. By comparing an impact strength of the PP/NH_2-SiO_2 composite with that ones containing compatibilizer, it is clear that the compatibilizer is critical for high toughness obtaining. On the basis on the above analysis, it is concluded that a synergetic toughening effect can be acquired when both NH_2-SiO_2 and EOC-*g*-GMA are present in PP matrix.

From Fig. 10 we see that, a yield point for all specimens is evident and almost unaffected by the addition of NH_2-SiO_2 nanoparticles. However, the addition of EOC-*g*-GMA slightly decreases tensile strength compared to neat PP. It could be expected when rubber-type grafted polymer such as ethylene/*n*-octene copolymer is introduced into PP/NH_2-SiO_2 composite. Additionally, stiffness is enhanced due to the higher tensile modulus (see Table 4). The maximum improvement in tensile modulus is 14 % achieved by the composite without compatibilizer. Since, the crystallinity and spherulite size of matrix in the PP/NH_2-SiO_2 composites is lower compared to neat PP, the increase in tensile modulus should be attributed to the rigid particles themselves. It is well known, that the improvement in the modulus depends on the morphology of composites [18, 32, 33]. Reinforcing efficiency of the nanofiller is balanced by two opposite phe-

T a b l e 4. Mechanical properties of PP and PP/NH_2-SiO_2 composites, differing in EOC-*g*-GMA content

Property	PP	PP/NH_2-SiO_2(98/2)/EOC-*g*-GMA (wt %)		
		0	4	6
Yield point, MPa	29.5 ± 0.08	28.7 ± 0.16	27.1 ± 0.02	26.3 ± 0.14
Elongation at break, %	53.6 ± 1.4	54.7 ± 1.1	82.1 ± 1.4	95.1 ± 1.0
Tensile modulus, MPa	1250 ± 14	1440 ± 13	1320 ± 10	1275 ± 8
Notched Charpy impact strength, kJ/m^2	15 ± 0.5	12 ± 0.1	16 ± 0.1	24 ± 0.3

nomena. The negative effect can be attributed to migration of nanoparticles into the interphase of nanoparticle-matrix causing worse performance. Dispersion of nanosilica as positive effect could enhance the modulus.

Correlating the crystalline behavior and mechanical properties of PP/NH_2-SiO_2 composites, one can conclude that the improvement in tensile properties of composites is mainly caused by the change of the stress state around the nanoparticles, because decreased crystallinity and spherulite size can only lead to decreased stiffness and strength [34]. Of course, the effect of crystalline behavior of matrix on the fracture toughness of a crystalline polymer is very complicated and needs to be further investigated.

CONCLUSIONS

The studies on the morphological, thermal and mechanical properties show that the addition of EOC-*g*-GMA to the surface modified nanosilica-filled polypropylene composites significantly improved the impact strength and elongation at break, and slightly decreases the tensile strength and tensile modulus, resulting in enhanced toughness. SEM observations showed that all the samples contain agglomerates. However, the tendency to form agglomerates decreases in the presence of EOC-*g*-GMA. Based on DSC results, it can be concluded that the crystalline features of PP have not been influenced greatly by addition of both modified silica nanoparticles and compatibilizer. However, the spherulite size of PP in all composites dramatically decreased compared to neat PP. The thermal stability of the composites was better compared to neat PP. Moreover, the thermal stability of the composites increases with increased compatibilizer content. From DMTA measurements, both storage modulus and loss modulus of all PP/NH_2-SiO_2 composites are significantly increased. However, the addition of compatibilizer slightly decreased stiffness of the composites. The glass transition temperature of matrix in all composites is greatly increased up to 6 °C.

It can be concluded that this approach can generate composites having a good balance of stiffness due to the reinforcement of the PP matrix in the presence of silica nanoparticles (NH_2-SiO_2), and toughness because of the presence of the dispersed rubber-type grafted polymer phase (EOC-*g*-GMA).

ACKNOWLEDGMENT

This work has been financially supported by project KB/146/13562/IT1-B/U/08 from the National Centre of Research and Development.

REFERENCES

[1] More E.P., Larson G.A.: "Polypropylene handbook", Hanser, Munich 1996.

[2] Qian J., Zhang H., Cheng G., Huang Z., Dang S., Xu Y.: *J. Sol-Gel. Sci. Technol*. **2010**, *56*, 300. http://dx.doi.org/10.1007/s10971-010-2306-6

[3] Dorigato A., Pegoretii A.: *J. Appl. Polym. Sci*. **2014**. http://dx.doi.org/10.1002/app.40242

[4] Barczewski M., Czarnecka-Komorowska D., Andrzejewski J., Sterzyński T., Dutkiewicz M., Dudziec B.: *Polimery* **2013**, *58*, 805. http://dx.doi.org/10.14314/polimery.2013.805

[5] "Optimization of polymer nanocomposite properties" (ED. Mittal V.), Wiley-VCH Verlang GmbH & Co. KGaA, Weinheim 2010.

[6] Lin H.O., Akil H.M., Ishak Z.A.M.: *Polym. Compos.* **2009**, *30*, 1693. http://dx.doi.org/10.1002/pc.20744

[7] Macan J., Brnardić I., Orilić S., Ivankowić H., Ivankowić M.: *Polym. Degrad. Stab.* **2006**, *91*, 122. http://dx.doi.org/10.1016/j.polymdegradstab.2005.04.024

[8] Bikiaris D.N., Vassilou A., Pavildou E., Karayannids C.P.: *Eur. Polym. J.* **2005**, *41*, 1965. http://dx.doi.org/10.1016/j.eurpolymj.2005.03.008

[9] Barus S., Zanetti M., Lazzari M., Costa L.: *Polymer* **2009**, *50*, 2595. http://dx.doi.org/10.1016/j.polymer.2009.04.012

[10] Lee J.H., Jung D., Hong C.E., Rhee K.Y., Advani S.G.: *Compos. Sci. Technol.* **2005**, *65*, 1996. http://dx.doi.org/10.1016/j.compscitech.2005.03.015

[11] Chen J.H., Rong M.Z., Ruan W.H., Zhang M.Q.: *Compos. Sci. Technol.* **2009**, *69*, 252. http://dx.doi.org/10.1016/j.compscitech.2008.10.013

[12] Hudgin D.E.: "Handbook of polypropylene and polypropylene composites", Marcel Dekker, New York 2003.

[13] Dougnac V.N., Alamillo R., Peoples B.C., Quijada R.: *Polymer* **2010**, *51*, 2918. http://dx.doi.org/10.1016/j.polymer.2010.02.014

[14] Lin H.O., Akil H.M., Ishak Z.A.M.: *Polym. Compos.* **2011**, *32*, 1568. http://dx.doi.org/10.1002/pc.21190

[15] Pustak A., Pucić I., Denac M., Svab I., Pohleven J., Musil V., Smit I.: *J. Appl. Polym. Sci*. **2013**, *128*, 3099. http://dx.doi.org/10.1002/app.38487

[16] *Pol. Pat.*198 188 (2008).

[17] Barthel H.: *Colloid Surf. A* **1995**, *101*, 217. http://dx.doi.org/10.1016/0927-7757(95)03179-H

[18] Jeziórska R., Świerz-Motysia B., Zielecka M., Szadkowska A., Studziński M.: *J. Appl. Polym. Sci.* **2012**, *125*, 4326. http://dx.doi.org/10.1002/app.36579

[19] *Pol. Pat.* 211 107 (2012).

[20] Jeziórska R., Świerz-Motysia B., Szadkowska A.: *Polimery* **2010**, *55*, 748.

[21] Zielecka M., Bujnowska E., Kępska B., Wenda M., Piotrowska M.: *Prog. Org. Coat.* **2011**, *72*, 193. http://dx.doi.org/10.1016/j.porgcoat.2011.01.012

[22] *Pol. Pat.* 198 188 (2007).

[23] Zielecka M., Bajdor K., Bujnowska E., Cyruchin K.: *Przem. Chem.* **2007**, *86*, 305.

[24] Jeziórska R.: *Int. Polym. Proc.* **2007**, *22*, 122. http://dx.doi.org/10.3139/217.0014

[25] Zapata P., Quijada R., Benavente R.: *J. Appl. Polym. Sci.* **2011**, *119*, 1771. http://dx.doi.org/10.1002/app.32888

[26] Osman A., Atallah A.: *Macromol. Chem. Phys.* **2007**, *208*, 87. http://dx.doi.org/10.1002/macp.200600435
[27] Zhou R., Burkhart T.: *J. Mater. Sci.* **2011**, *46*, 1228. http://dx.doi.org/10.1007/s10853-010-4901-x
[28] Jeziórska R., Zielecka M., Gutarowska B., Żakowska Z.: *Int. J. Polym. Sci.* **2014**. http://dx.doi.org/10.1155/2014/183724
[29] Rong M.Z., Zhung M.Q., Pun S.L., Lehmann B., Friedrich K.: *Polym. Int.* **2004**, *53*, 176. http://dx.doi.org/10.1002/pi.1307
[30] Benavente R., Perez E., Yazdani-Pedram M., Quijada R.: *Polymer* **2002**, *43*, 6821. http://dx.doi.org/10.1016/S0032-3861(02)00611-0
[31] Paul S.A., Sinturel C., Joseph K., Gen M.G.D., Pothan L.A., Thomas S.: *Polym. Eng. Sci.* **2010**, *50*, 384. http://dx.doi.org/10.1002/pen.21522
[32] Jeziórska R., Świerz-Motysia B., Zielecka M., Studziński M.: *Polimery* **2009**, *54*, 647.
[33] Vladimirov V., Betchev C., Vassiliou A., Papageorgiou G., Bikiaris D.: *Compos. Sci. Technol.* **2006**, *66*, 2935. http://dx.doi.org/10.1016/j.compscitech.2006.02.010
[34] Way J.L., Atkinson J.R., Nutting J.: *J. Mater. Sci.* **1974**, *9*, 293. http://dx.doi.org/10.1007/BF00550954